Heat-Transfer Enhancement Using Weakly Ionized, Atmospheric Pressure Plasma in Metallurgical Applications

V. RAJAMANI, R. ANAND, G.S. REDDY, J.A. SEKHAR, and M.A. JOG

Experimental measurements and computational analysis of heat transfer in atmospheric pressure, midtemperature range (1200 to 1600 K) plasma flow over an aluminum cylinder have been carried out. A comparison of transient temperature measurements for the aluminum cylinder under convective unionized air flow and those with convective plasma flow shows significantly higher heat transfer from plasma flow compared to air flow under identical temperature and flow conditions. A heat-transfer problem is computationally modeled by using available experimental measurements of temperature rise in the cylinder to determine the degree of ionization in the plasma flow. The continuity, momentum, and energy conservation equations, as well as conservation equations for electrons and ions, and the Poisson's equation for self-consistent electric field are solved in the plasma by a finite volume method. The conjugated transient heat transfer in the cylinder and in the plasma is obtained by simultaneous solution of the transient energy conservation equations. It is shown that the enhancement of heat transfer in plasma flow is due to the energy deposited by charged species during recombination reaction at the solid surface. An important finding is that even a small degree of ionization (<1 pct) provides significant enhancement in heat transfer. This enhancement in heat transfer can lead to a productivity increase in metallurgical applications.

I. INTRODUCTION

THE flow of plasma, or ionized gas, is used in a variety of materials processing and metallurgical applications including plasma spray coating, arc welding, near-net-shape manufacturing, plasma vapor deposition, polymer deposition, and wire bonding in microelectronic chips.[1,2] Based on the temperature and pressure range, the plasmas used in these applications can be divided in two primary types. First are the systems that use high temperature and atmospheric or near-atmospheric pressure ionized gas, also referred to as thermal plasmas. The condition of local thermodynamic equilibrium (LTE) is reached in thermal plasma with temperatures around 10,000 K and electron densities ranging from 10^{21} to 10^{26} m^{-3}. The high temperatures prevalent in thermal plasmas are useful for heating and melting of ceramic and metallic particles in coating and welding applications and in destruction of bio-hazardous materials. The second type of systems use the low-pressure, low-temperature plasmas. The operating pressure and gas density are very low. There is a significant difference in electron and heavy particle (neutral and ions) temperature due to the weak collision coupling between them. The temperature of ions and neutral molecules is typically close to room temperature. The abundance of ionized species in this type of plasma is used to aid in chemical reactions in vapor deposition and polymer processing.

V. RAJAMANI, formerly Research Assistant with the Department of Mechanical Engineering, University of Cincinnati, is Research Engineer, Saint Gobain R&D Centre, Northborough, MA 01532. R. ANAND, formerly Research Assistant with the Department of Mechanical Engineering, University of Cincinnati, is Design Engineer, Caterpillar Corporation, Peoria, IL 61614. G.S. REDDY, Scientist, is with M.H.I. Inc., Cincinnati, OH 45215. J.A. SEKHAR, Professor, Department of Chemical and Materials Engineering, and M.A. JOG, Associate Professor of Mechanical Engineering, Department of Mechanical Engineering, are with the University of Cincinnati, OH 45221-0072. Contact e-mail: millind.jog@uc.edu

Manuscript submitted November 28, 2005.

In the 1960s and 1970s, heat transfer in plasma flow received much attention in the literature, mainly in the context of electrostatic probes and aerospace applications, whereas in the last 30 years, the attention has primarily focused on plasma flow as it relates to plasma-aided manufacturing. Available reviews[3,2] provide detailed discussion of a number of factors that affect the heat transfer to a solid body from plasma. It is noted that the analysis of heat transfer from plasma to a solid surface is significantly more complicated as compared to unionized gas flow, because it not only involves the hydrodynamic and thermal boundary layers encountered in unionized gas flows, but also the electrical effects due to the presence of charged species. These electrical effects arise due to the difference in mobilities of the ion and the electron. The electrons having very high mobility travel faster toward the surface and give rise to a negative potential at the solid surface.[4] This negative potential repels electrons and attracts ions. Subsequently, the flow of ions and electrons toward the surface becomes equal and the surface potential remains constant thereafter. The surface potential when both the ion and electron fluxes become equal is called the floating potential.[4] These charged species recombine at the surface and release energy equivalent to their ionization potential to the surface. Therefore, the electric field and charged species transport play an important role in determining the heat transport to the surface.[2,3,5,6]

Atmospheric pressure, high-temperature thermal plasmas have been studied extensively. Review[7] and a monograph[3] provide detailed discussion of the work published in the literature. Heat and momentum transfer to spherical particles in thermal plasma has been studied extensively for the application of plasma spray coating (Reference 7 and references therein). A unified treatment of heat transfer under continuum and noncontinuum conditions has been developed.[8] Correlations for Nusselt number have been proposed for thermal plasma flow over spherical particles.[9]

These correlations have been employed by several researchers in computational analysis of plasma spray systems (for example, Proulx *et al.*[10]). However, these correlations ignore the electrical effects. For plasmas at low pressure, heat transfer to a solid has been investigated applying results from kinetic theory of rarefied gases.[11,12]

Unfortunately, these two extremes (very hot plasmas at atmospheric pressure or cold plasmas at low pressures) are not best suited for common metallurgical work. For example, most of the aluminum melting or steel heat treatment is carried out between 900 and 1500 K. The low-pressure plasma possesses very low-energy density and cannot be used for aluminum melting. The very high-temperature thermal plasmas result in significant heat losses and may result in poor efficiencies. Only recently, atmospheric pressure convective plasma torches have become available that provide midtemperature range plasma (1200 to 1600 K) at atmospheric pressure. These plasma torches are being considered for aluminum melting, continuous flow plasma chemical reactors, surface heat treatment, and remediation of biohazards and toxic wastes. However, plasma flows under these conditions are not yet well characterized. To design and improve midtemperature plasma devices, the ability to predict the plasma flow over a solid body and the concomitant heat transfer is highly desirable.

In this article, we report experimental measurements of temperature rise in an aluminum cylinder exposed to air flow and plasma flow under identical temperature and flow conditions. The results show significant increase in heat transfer with plasma flow. Computational modeling for air flow and plasma flow has been carried out to determine the degree of ionization in the plasma and to analyze the heat-transfer phenomena in the two cases.

A. *Experimental Setup*

A schematic of the experimental setup is shown in Figure 1. The setup consists of an insulated cylindrical chamber. An AIRTORCH* or a PLASMA AIRTORCH* is connected to the chamber on the left and the high-temperature gas enters the chamber through the opening along the centerline of the chamber. A thermocouple is placed at the entrance of the chamber to measure the temperature at the exit of the torch. An aluminum sprue is placed in the chamber with a thermocouple attached to the sprue through a hole drilled from the back of the sprue along its centerline. The thermocouple is at a location 12 mm from the front surface along the centerline. The K-type thermocouple was used, which can record temperatures up to 1500 K. The air torch exit temperature was measured with a B-type thermocouple. Both thermocouples were connected to a data acquisition system for transient temperature measurements. An MHI data acquisition system was employed for the thermal measurements, and the sampling rate was 1 Hz. The mass flow rate was measured at the inlet and the average velocity at the inlet of the insulated chamber was calculated based on the measured temperature.

*AIRTORCH and PLASMA AIRTORCH are trademarks of MHI Inc., Cincinnati, OH.

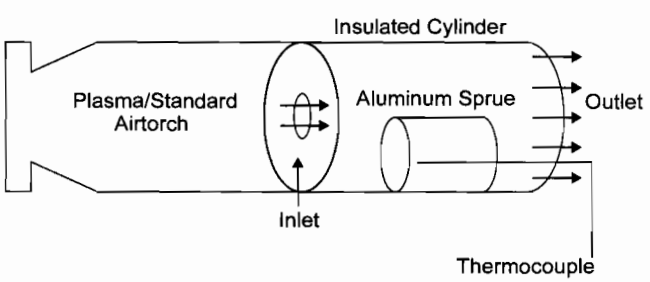

Fig. 1—A schematic of the experimental setup.

Temperature measurements were carried out with two identical aluminum sprues of 38.7-mm diameter and 39-mm length. In the first case, an air torch was used to provide the gas at 1573 K for convectively heating the sprue. Transient temperature measurements were recorded. In the second case, a plasma torch was used. In this case, a weakly ionized gas from the torch provided the convective heating of the sprue. Once again, a transient temperature change was measured for the sprue interior. The sprue heated with the plasma torch resulted in a substantially higher heating rate compared to the one heated with the air torch. The experimental measurements are discussed in Section II–B, in detail, with the computational predictions.

B. *Computational Analysis*

A flow of weakly ionized gas consisting of neutrals, ions, and electrons over a cylindrical aluminum sprue is considered. The far-field pressure is atmospheric and the flow Reynolds number based on the inlet velocity and sprue diameter is in the laminar range. Because the degree of ionization is expected to be small, the overall velocity field can be found from the solution of the continuity, momentum, and energy equations for the neutral gas flow field.[13] The flow was considered to be steady and axisymmetric; however, the temperature field was considered transient due to heating of the sprue. Gas thermophysical properties were evaluated at the far-field temperature. The neutral gas flow in the chamber and conduction in the sprue were computationally modeled by using a FLUENT 6.2.1 (Fluent Inc., Lebanon, NH) commercial flow/thermal solver. Using GAMBIT 2.1 (Fluent Inc., Lebanon, NH), a two-dimensional axisymmetric mesh was generated using the dimensions given in the experimental setup. The mesh generated was highly refined in order to facilitate greater accuracy in the numerical solution and to account for steep gradients near the sprue.

Using the velocity field, a computational model was developed to evaluate the electron and ion flux and the self-consistent electric field. A separate program was developed to determine the number density of charged species and the electric field, as described subsequently. The charged species flux to the surface was then evaluated and the contribution to heat transfer due to recombination of electrons and ions was determined.

Using the dimensionless quantities $u^* = u/U_\infty$, $p^* = p/\rho U_\infty^2$, $T^* = T/T_\infty$, $t = tU_\infty/R$, $V^* = eV/(kT_\infty)$, $N^*_{e,i} = N_{e,i}/N_o$, $T^*_{e,i} = T_{e,i}/T_\infty$, $Sc_i = \nu/D_i$, $\beta = D_i/D_e$, $Re = 2U_\infty R/\nu$, $\Gamma^*_{e,i} = \Gamma_{e,i}eR/(\mu_{e,i}N_o kT_\infty)$, $Pr = \nu/\alpha$, $\lambda_D = [\varepsilon_0 kT_\infty/e^2N_o)]^{1/2}$, and $\varepsilon = \lambda_D/R$, the governing equations in dimensionless form are as follows.

Mass conservation:

$$\nabla^* u^* = 0 \quad [1]$$

Momentum conservation:

$$u^* \nabla^* u^* = -\nabla^* p^* + \frac{2}{\mathrm{Re}} \nabla^{*2} u^* \quad [2]$$

Energy conservation in the plasma:

$$\frac{\partial T^*}{\partial t^*} + u^* \nabla^* T^* = \frac{2}{\mathrm{Re\,Pr}} \nabla^* (\nabla^* T^*) \quad [3]$$

Energy conservation in the sprue:

$$\frac{\partial T_s^*}{\partial t^*} = \frac{2(\alpha_s/\alpha)}{\mathrm{Re\,Pr}} \nabla^* (\nabla^* T_s^*) \quad [4]$$

Neglecting production and recombination of the charged species in the bulk of the flow, the conservation equations for the charged species number densities and the governing equation of the self-consistent electric field can be written as follows.

Continuity equations for electrons:

$$\frac{\beta \mathrm{ReSc}_i}{2} u^* \nabla^* N_e^* - \nabla^{*2} (N_e^* T_e^*) + \nabla^* N_e^* \nabla^* V^* = 0 \quad [5]$$

Continuity equations for ions:

$$\frac{\mathrm{ReSc}_i}{2} u^* \nabla^* N_i^* - \nabla^{*2} (N_i^* T_i^*) - \nabla^* N_i^* \nabla^* V^* = 0 \quad [6]$$

Poisson equation for electric field:

$$\varepsilon^2 \nabla^{*2} V^* = (N_e^* - N_i^*) \quad [7]$$

The ion and electron fluxes are given by

$$\begin{aligned} \Gamma_e^* &= -\nabla (N_e^* T_e^*) + N_e^* \nabla^* V^* \\ \Gamma_i^* &= -\nabla (N_i^* T_i^*) - N_i^* \nabla^* V^* \end{aligned} \quad [8]$$

The plasma and air are considered optically thin and the radiation transport is considered between the sprue surface and the container wall. Since the gas is at atmospheric pressure, the difference in temperature between the neutral gas and the charged species was assumed to be small throughout the flow domain ($T \approx T_i \approx T_e$).

The flow field for the computational domain is obtained first by solving Eqs. [1] and [2] in the FLUENT flow/thermal solver. The SIMPLE algorithm for pressure correction was employed and discretization was carried out using the Power-law method, as described in Patankar.[14] An under-relaxation technique was used for the momentum equation. The solution of these equations provides the flow field in the entire domain. Equations [3] through [7] are solved to obtain the number density distribution of the ions and electrons and the electric potential in the plasma as well as temperature distributions in the plasma and the sprue. A finite difference method was employed to discretize Eqs. [3] through [7] based on the alternate direction implicit scheme.[14] A computer program was developed to iteratively solve the resulting tridiagonal systems of equations using the Thomas algorithm. We expect to have steep gradients in velocity and temperature near the sprue surface. To resolve these steep variations, a very fine grid was taken. The convergence criterion was set at 1×10^{-6} of relative error between successive iterations at all points. Thermophysical properties for charged species were obtained from References 3 and 15. For the case of heating from unionized air flow, the methodology is similar to the one described previously; however, Eqs. [5] through [7] are not needed.

C. *Boundary Conditions*

The governing equations were solved with the following boundary conditions. The sprue surface was considered as a perfect sink for the charged species $N_i^* = N_e^* = 0$. The sprue surface was considered at the floating potential so that $\Gamma_e = \Gamma_i$. The velocity was zero due to the no-slip condition at all solid surfaces. The heat balance at the surface is $-\chi \frac{\partial T}{\partial n} + q''_{\text{recombination}} + q''_{\text{radiation}} = -\chi_s \frac{\partial T_s}{\partial n}$. The heat flux deposited at the surface due to charged species recombination is given by $q''_{\text{recombination}} = \Gamma_e V_i$. At the inlet, $T_i = T_e = T_\infty$ and the inlet velocity is specified. At the walls of the outer chamber, temperature and electric potential gradients are zero and velocity is zero. At the outlet, the outflow condition of the zero gradient of temperature in the axial direction is considered. The zero gage pressure is prescribed at the outlet.

II. RESULTS AND DISCUSSION

In a computational study, it is important to evaluate the effect of grid spacing on the solutions to make sure that the results are grid independent. The computations were carried with different grid sizes until the solution was insensitive to the grid size. The node points were doubled until the computed heat-transfer coefficient at the sprue surface changed by less than 0.1 pct. The final grid had 721 points in the axial direction and 193 points in the radial direction.

A. *Heat Transfer in Air Flow*

Using this grid, we first considered the flow from an air torch in the analysis. The streamlines for the flow are shown in Figure 2. It is clear from the figure that as the flow goes around the sprue, a recirculating flow pattern is obtained. Due to the decrease in the cross-sectional area due to the presence of the sprue, the velocity increases as the gas moves along the container walls.

The temperature contours obtained for the flow domain are shown in Figure 3. In most of the region in the upstream of the sprue, the temperature is nearly uniform. Due to the recirculating vortex patterns on the downstream region from the sprue, colder fluid from the sprue mixes with the hotter fluid away from the sprue. This is evident from the temperature contours. The temperature contours show

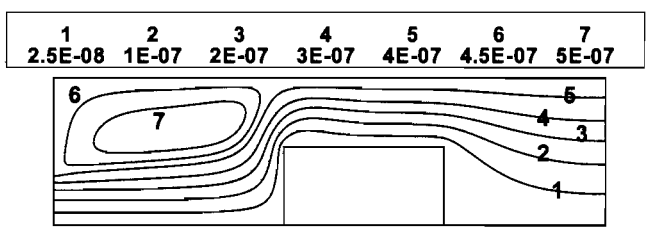

Fig. 2—Flow stream lines.

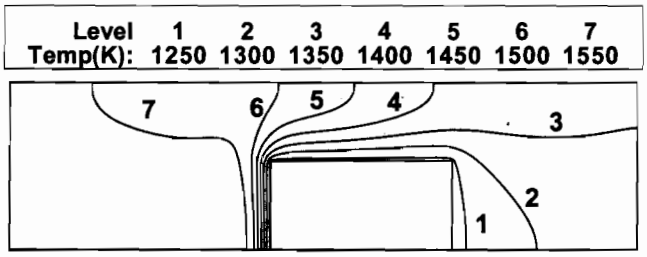

Fig. 3—Temperature contours with air torch heating (K).

that the heat-transfer rate is maximum at the front surface of the sprue as there is a sharp change in gas temperature near the surface. As the flow proceeds toward the outlet, there is a decrease in the heat-transfer rate on the top surface of the sprue. This is evident from the temperature contours showing the temperature drop over a larger distance compared to the front surface. The heat-transfer coefficient was obtained at all points along the surface of the sprue by equating the net heat transfer to the surface from gas flow to the product of heat-transfer coefficient and the temperature difference between the inlet temperature and the surface temperature as $-\chi \partial T/\partial n + q''_{\text{recombination}} + q''_{\text{radiation}} = h(T_\infty - T_s)$. Then, the overall heat-transfer coefficient was obtained by an area weighted average taken over the surface of the sprue. The temperature contours in the interior of the sprue showed only a small variation. This is to be expected due to the high thermal conductivity of aluminum (χ_s = 227 W/m K). The Biot number is very low and the temperature distribution is nearly uniform.

B. *Heat Transfer in Plasma Flow*

With plasma flow, number densities of charged species and the induced electric field are determined. Figures 4(a) and (b) show the dimensionless ion and electron density contours, respectively, with the degree of ionization at the inlet as 0.64 pct. The motion of the charged species is the net effect of convection, diffusion, and drift under the influence of electric field. Both ion and electron are convected with the same neutral flow. However, the electric field has an opposite effect on the motion of ions as compared to that of electrons. Because the electric potential at the surface is negative, it results in repelling electrons and attracting ions. Not surprisingly, the number densities of electrons are low closer to the surface, whereas ion densities are higher near the sprue surface. The recombination reaction of charged species at the surface gives energy equal to the ionization potential to the surface.

Figure 5 shows the transient temperature measurement with the thermocouple placed in the sprue interior. The significant increase in the rate of temperature rise indicates higher heat transfer with plasma heating as compared to heating with air flow. To validate our model, we first compared the computational results of the temperature rise with Airtorch heating to experimental measurements. As seen in the figure, the computational results match well with the experimental measurements. Next, to determine the degree of ionization in plasma, a parametric study was conducted by considering different values of inlet ion and electron number

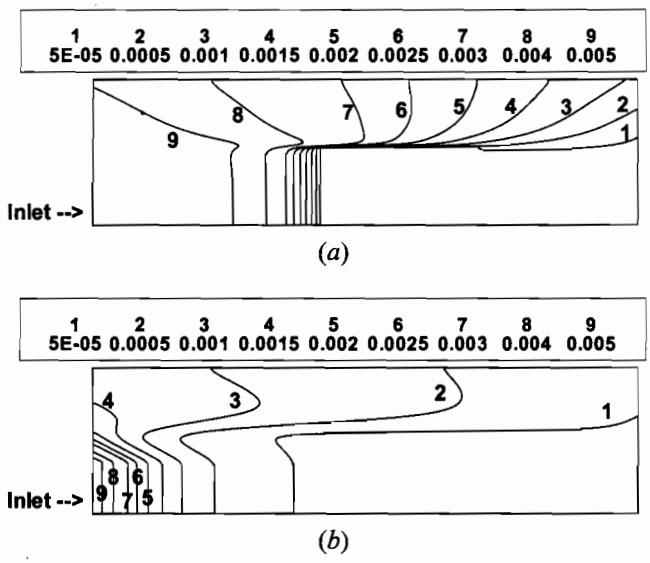

Fig. 4—(*a*) Dimensionless ion number density contours and (*b*) dimensionless electron number density contours.

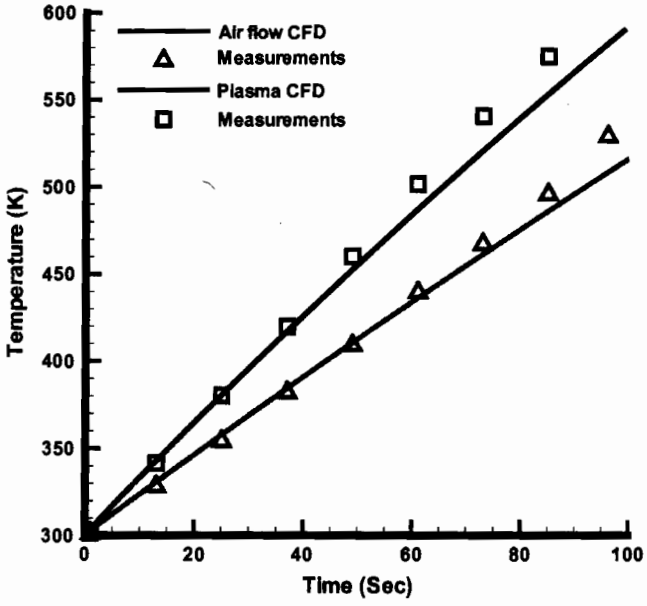

Fig. 5—Comparison of computational predictions and experimental measurements of temperature increases in the sprue.

densities. The predicted values of the temperature rise with different degrees of gas ionization were compared with the experimental measurements of temperature change in the sprue interior with plasma heating. This gave the degree of ionization as 0.64 pct for the case considered here. The predicted results for 0.64 pct ionization are shown in Figure 5.

The influence of ionization on heat-transfer enhancement is plotted in Figure 6. The figure shows the area weighted average heat-transfer coefficient as a function of the degree of ionization at the inlet. With an increase in the degree of ionization, the number densities of charged species and hence the flux of charged species to the sprue surface increases. This leads to higher heat transfer to the sprue

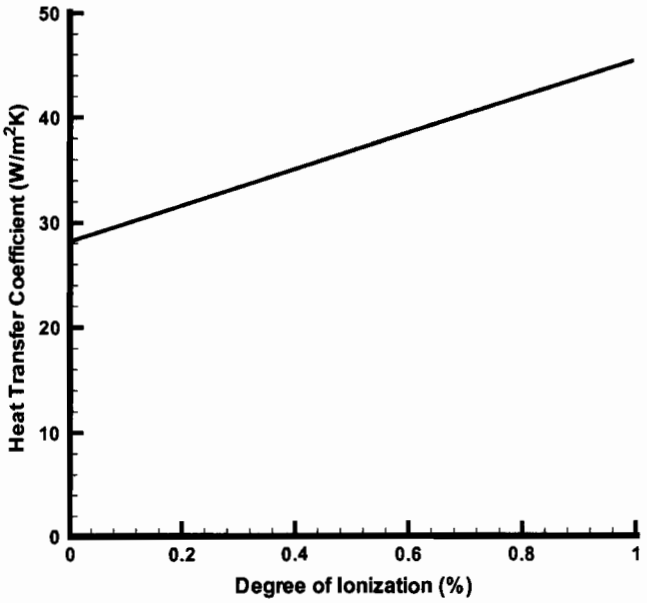

Fig. 6—Variation of heat-transfer coefficient with the degree of ionization.

surface and the enhancement of heat transfer is seen to increase nearly linearly with the degree of ionization. For the first case with no ionization, the average heat-transfer coefficient was 28.2 W/m^2 K, whereas with plasma flow with 0.64 pct ionization, the heat-transfer coefficient was 39.2 W/m^2 K. A change in the gas ionization from 0 to 0.64 pct resulted in an approximately 40 pct increase in the average heat-transfer coefficient. It may be noted that the model presented here is restricted to weakly ionized gas, and as such, the results should not be directly extrapolated beyond 1 pct ionization unless field effects are incorporated.

III. SUMMARY AND CONCLUSIONS

Transient temperature measurements and computational simulation of convective heating of an aluminum sprue were carried out. Two cases were considered, one with heating by unionized air flow and the other with plasma flow. The transient temperature rise in the sprue interior was measured, and it showed a significant increase in heat transfer with plasma flow compared to air flow under identical temperature and flow conditions. To computationally simulate the process, the flow of continuum, axisymmetric, laminar, and midtemperature range (1200 to 1600 K) plasma over a cylinder was modeled using a finite volume method. The continuity and the momentum conservation equations for the flow were solved using the commercially available FLUENT flow/thermal solver. Using the flow field, a computational model was developed to solve the governing equations for the conservation of electrons and ions and the self-consistent electric field as well as the energy conservation in the gas flow and the sprue interior. The governing equations were discretized using a finite volume method and the resulting system of equations was solved by the alternating direction implicit scheme. Transient heat transfer to the cylinder was evaluated by considering convective heat transfer from the neutral flow, the energy transport by radiation between the sprue surface and the wall, and the energy deposited by recombination of charged species at the cylinder surface. Results for transient temperature rise in the cylinder with air heating were used to validate the computational model. The degree of ionization present in the plasma flow was determined. The following conclusions can be drawn from this study.

1. The heat transfer to a solid surface is higher when exposed to the atmospheric, midtemperature range plasma flow compared to the flow of unionized air at identical flow and temperature conditions.
2. The heat-transfer enhancement is due to the ionization energy deposited by charged species due to their recombination at the surface.
3. Even a small degree of ionization (less than 1 pct) can lead to significant enhancement in heat transfer.

NOMENCLATURE

D	diffusivity (m^2/s)
e	electron charge (C)
h	heat-transfer coefficient (W/m^2 K)
k	Boltzmann constant (J/K)
m	mass (kg)
N	number density (1/m^3)
p	pressure (Pa)
Pr	Prandtl number
q	heat-transfer rate (W)
q''	heat flux (W/m^2)
r	radial coordinate (m)
R	radius (m)
Re	Reynolds number
Sc	Schmidt number
T	temperature (K)
t	time (s)
u	velocity (m/s)
V	voltage (V)
x	axial coordinate (m)

Greek letters

α	thermal diffusivity (m^2/s)
Γ	flux of ions and electrons (1/m^2)
β	ratio of ion to electron diffusivity
μ	viscosity (Ns/m^2)
μ_{ei}	mobility (m^2/Vs)
ρ	density (kg/m^3)
χ	thermal conductivity (W/m K)

Subscripts

i	ion
e	electron
w, s	wall
∞	inlet

REFERENCES

1. R.W. Smith, D. Wei, and D. Apelian: *Plasma Chem. Plasma Processing*, 1989, vol. 9, pp. 135-65.
2. P.S. Ayyaswamy and I.M. Cohen: *Annual Review of Heat Transfer—Vol. 12*, Hemisphere Publishing, New York, NY, 2002, pp. 27-78.

3. M.I. Boulos, P. Fauchais, and E. Pfender: *Thermal Plasmas: Fundamentals and Applications*, Plenum Press, New York, NY, 1994, vol. 1, pp. 22-43.
4. S.R. Sheshadri: *Fundamentals of Plasma Physics*, Elsevier Publishing, New York, NY, 1973, pp. 76-83.
5. M.A. Hader and M.A. Jog: *Phys. Plasmas*, 1998, vol. 5, pp. 902-09.
6. M.A. Jog and L. Huang: *J. Heat Transfer*, 1996, vol. 118, pp. 471-77.
7. Y.P. Chyou and E. Pfender: *Plasma Chem. Plasma Proc.*, 1989, vol. 9, pp. 45-71.
8. E. Laveroni and E. Pfender: *Int. J. Heat Mass Transfer*, 1990, vol. 33, pp. 1497-509.
9. R.M. Young and E. Pfender: *Plasma Chem. Plasma Proc.*, 1987, vol. 7, pp. 211-26.
10. P. Proulx, J. Mostaghimi, and M. Boulos: *Int. J. Heat Mass Transfer*, 1985, vol. 28 (7), pp. 1327-36.
11. X. Chen: *J. Phys. D: Appl. Phys.*, 1997, vol. 30, pp. 1885-92.
12. A.G. Gnedovets and A.A. Uglov: *Plasma Chem. Plasma Proc.*, 1992, vol. 12, pp. 383-401.
13. P.M. Chung, L. Talbot, and K.J. Touryan: *Electric Probes in Stationary and Flowing Plasmas: Theory and Applications*, Spinger, Berlin, 1975, pp. 39-78.
14. S.V. Patankar: *Numerical Heat Transfer and Fluid Flow*, Hemisphere Publishing, New York, NY, 1980, pp. 79-131.
15. S.C. Brown: *Basic Data of Plasma Physics*, MIT Press, Cambridge, MA, 1966, pp. 88-89.